Diarylethane α-chloroester ferroelectric liquid crystals

H. T. Nguyen[a]; A. Babeau[a]; C. Léon[a]; J. -P. Marcerou[a]; C. Destrade[a]; A. Soldera[b]; D. Guillon[b]; A. Skoulios[b]

[a] Centre de Recherche Paul Pascal, Pessac, France [b] Groupe de Matériaux Organiques, Institut de Physique et Chimie, Strasbourg, Cedex, France

PLEASE SCROLL DOWN FOR ARTICLE

Diarylethane α-chloroester ferroelectric liquid crystals

by H. T. NGUYEN*, A. BABEAU, C. LÉON,
J.-P. MARCEROU and C. DESTRADE

Centre de Recherche Paul Pascal, Château Brivazac,
33600 Pessac, France

A. SOLDERA, D. GUILLON and A. SKOULIOS

Groupe de Matériaux Organiques, Institut de Physique et Chimie,
des Matériaux de Strasbourg, ICS, 6, rue Boussingault,
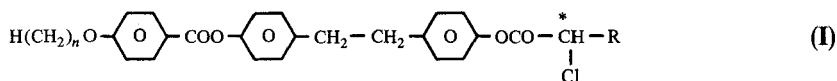67083 Strasbourg Cedex, France

Four new chiral diarylethane α-chloroester series have been synthesized and studied. All of the derivatives are mesogenic and display a ferroelectric S_C^* phase. In addition to this S_C^* phase, some of them exhibit other ferroelectric S_I^* and/or S_F^* phases. Transition temperatures and enthalpies are reported. Several electrooptical properties such as the spontaneous polarization and response times are given and discussed. Layer thickness and tilt angle in the smectic S_C^* phases of series **II** compounds were determined by X-ray diffraction.

1. Introduction

Since the electrooptic properties of ferroelectric chiral smectic C materials [1] were reported by Clark and Largerwall [2] in 1980 and by Yoshino and Ogaki [3] in 1984, the search to find new materials has increased and studies from both fundamental and practical points of view have been undertaken. In order to optimize the physical properties of ferroelectric liquid crystal mixtures, two general strategies to constitute the ferroelectric medium have been developed. In the first, a polar chiral compound is used as a dopant in a low viscosity smectic C mixture with a wide temperature range. The second consists of mixing several ferroelectric S_C^* materials with low viscocities. The flexible 1,2-diarylethane core, well known to induce tilted smectic phases [4], is quite adapted to obtain wide S_C temperature range, low viscosity mixtures as well as pure chiral smectic C* materials [5, 6].

In this paper, we report the synthesis, characterization and electrooptical properties of two homologous series of compounds having the general formulae

$$H(CH_2)_nO-\langle O \rangle-COO-\langle O \rangle-CH_2-CH_2-\langle O \rangle-OCO-\overset{*}{\underset{Cl}{CH}}-R \qquad (I)$$

and

$$H(CH_2)_nO-\langle O \rangle-CH_2-CH_2-\langle O \rangle-OOC-\langle O \rangle-OCO-\overset{*}{\underset{Cl}{CH}}-\underset{CH_3}{CH}-CH_3 \qquad (II)$$
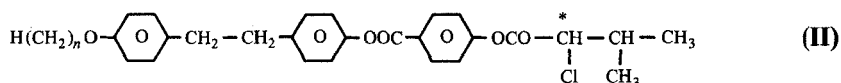
* Author for correspondence.

where

$$n = 6\text{--}12$$

$$R = CH_3\text{--}\overset{*}{CH}\text{--}(A), \quad C_2H_5\text{--}\overset{*}{CH}\text{--}(B)$$
$$\underset{CH_3}{\mid} \qquad\qquad \underset{CH_3}{\mid}$$
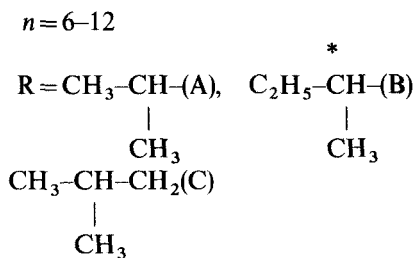
$$CH_3\text{--}CH\text{--}CH_2(C)$$
$$\underset{CH_3}{\mid}$$

2. Results and discussion

2.1. *Synthesis*

The compounds of series **I** and **II** were prepared according to the scheme:
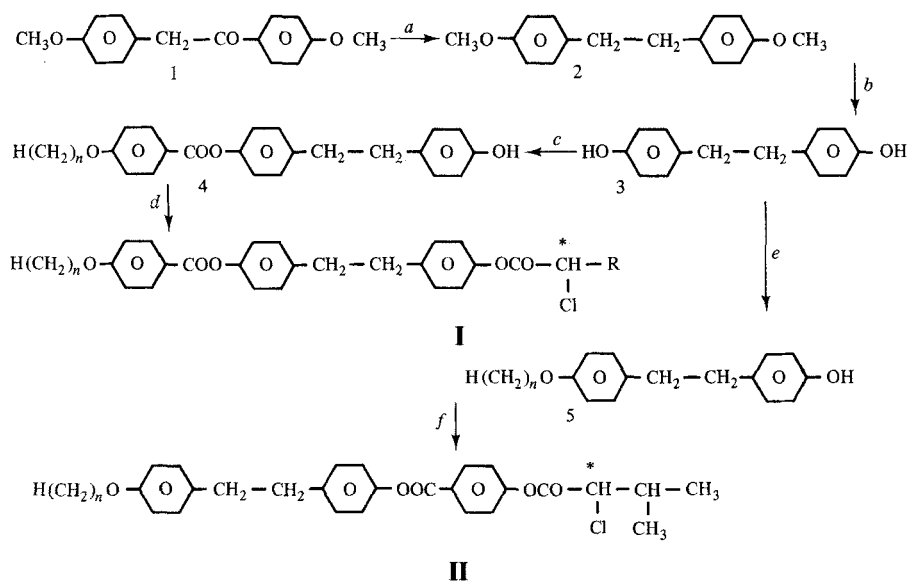
(a) KOH, NH_2–NH_2, DEG;

(b) *pyridine*, HCl, Δ;

(c) $H(CH_2)_nO$–Ph–COCl, *pyridine*;

(d) R–$\overset{*}{CH}$–COOH, DCC, DMAP;
$\qquad\quad \underset{Cl}{\mid}$

(e) $H(CH_2)_n$–Br, KOH, EtOH;

(f) CH_3–CH–CH–COO–Ph–CO_2H, DCC, DMAP.
$\qquad\quad \underset{CH_3}{\mid}\;\; \underset{Cl}{\mid}$

All of the final compounds were purified by chromatography on silica gel with toluene as eluent and were recrystallized from absolute ethanol. They form ferroelectric S_C^* phases. The liquid crystal transition temperatures and enthalpies of four homologous series **IA**, **B**, **C** and **II** are given in tables 1 (A), (B), (C) and 2.

2.2. *Optical microscopy studies*

2.2.1. *Series IA*

It can be seen from table 1 (A) that the clearing points (N*–I or S_A–I) and the melting temperature of the esters derived from L-valine, are almost independent of the chain length. The two first members of the series ($n = 6, 7$) do not display a S_A phase but exhibit N* and three different ferroelectric smectic phases namely S_C^*, S_I^* and S_F^*. The octyloxy derivative has to be pointed out, since it exhibits five mesomorphic phases: N*, S_A, S_C^*, S_I^* and S_F^*. On cooling from the isotropic liquid, the cholesteric phase appears with an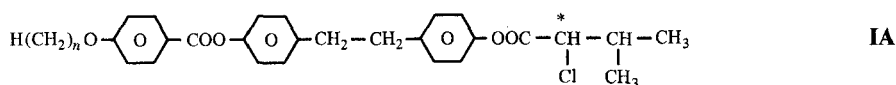 oily streak texture (see figure 1 (*a*)), and further cooling leads to the homeotropic and focal conic textures of the S_A phase (see figure 1 (*b*)). Below the S_A phase, three ferroelectric S_C^*, S_I^*, S_F^* phases appear successively with similar broken fan shaped and schlieren textures (see figures 1 (*c*), (*d*), (*e*)). As soon as $n = 9$ the S_F^* phase disappears and from $n = 10$ to $n = 12$, only three phases are observed: S_A, S_C^* and S_I^*. It has to be stressed here, that the two compounds ($n = 8, 9$) exhibit the required liquid crystal mesophases (S_C^*, S_A, N*) for display device applications.
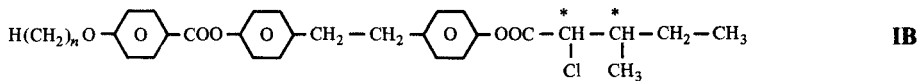
2.2.2. *Series IB*

As in series **IA**, the melting and clearing temperatures of series **IB**, derived from L-isoleucine do not change with chain length. If the melting point is the same in these two series, the clearing points of **IB**, on the other hand, are 10° lower than those of **IA** (see table 1 (B)). The first three members ($n = 6$–8) of this series do not form the S_A phase but in addition to N*, S_C^*, S_I^* (except for the hexyloxy derivative) they exhibit a more ordered and tilted S_J^* or S_G^* phase with a mosaic texture. The S_A phase only exists for $n = 9$–11. The S_I^* phase is enantiotropic for $n = 12$ while it is monotropic from $n = 7$ to $n = 11$. In this series only one compound ($n = 9$) has the desired sequence S_C^* S_A N* for display device applications.

Table 1. (A) Transition temperatures (°C) and enthalpies (kJ/mol) of compounds **IA**.

$$\text{H(CH}_2)_n\text{O}-\bigcirc-\text{O}-\text{COO}-\bigcirc-\text{O}-\text{CH}_2-\text{CH}_2-\bigcirc-\text{O}-\text{OOC}-\overset{*}{\underset{\underset{\text{Cl}}{|}}{\text{CH}}}-\underset{\underset{\text{CH}_3}{|}}{\text{CH}}-\text{CH}_3 \qquad \textbf{IA}$$

n	C		S_F^*		S_I^*		S_C^*		S_A		N*		I
6	•	84	•	88	•	92	•	116	—		•	137	•
		19·54		*0·235*		*2·28*		*0·30*				*1·68*	
7	•	86	•	87	•	94	•	122	—		•	135	•
		16·5		*0·119*		*2·05*		*0·193*				*1·82*	
8	•	84	•	85	•	95	•	128	•	130·5	•	137	•
		21·12		*0·026*		*1·95*		*0·031*		*0·234*		*2·11*	
9	•	85	—		•	95	•	130	•	133	•	135	•
		19·26				*1·64*		*0·034*		*0·99*		*2·29*	
10	•	84	—		•	95	•	131·5	•	136	—		•
		24·7				*1·87*		*0·033*		*7·06*			
11	•	85	—		•	95	•	132	•	135	—		•
		26·0				*1·76*		*0·016*		*7·14*			
12	•	84	—		•	94	•	133	•	133	—		•
		27·88				*1·94*		*0·015*		*8·43*			

Table 1. (B) Transition temperatures (°C) and enthalpies (kJ/mol) of compounds **IB**.

$$H(CH_2)_n O - \bigcirc - COO - \bigcirc - CH_2 - CH_2 - \bigcirc - OOC - \overset{*}{C}H - \overset{*}{C}H - CH_2 - CH_3$$
$$\underset{Cl}{|} \quad \underset{CH_3}{|}$$

IB

n	C		S_J^*		S_I^*		S_C^*		S_A		N*		I
6	●	82 *21·4*	●	(70) *0·97*	—		●	106 *0·294*	—		●	126 *1·23*	●
7	●	80 *20·9*	●	(66)	●	(79) *0·92*	●	112 *0·33*	—		●	125 *1·39*	●
8	●	77 *18·2*	●	(57)	●	(76) *0·90*	●	117 *0·12*	—		●	125 *1·91*	●
9	●	80 *22·1*	—		●	(77) *0·96*	●	118·5 *0·14*	●	120·5 *1·46*	●	122 *2·64*	●
10	●	82 *27·2*	—		●	(78) *1·06*	●	122 *0·07*	●	125 *5·65*	—		●
11	●	78 *27·3*	—		●	(77) *1·07*	●	124 *0·095*	●	125 *6·25*	—		●
12	●	78 *27·0*	—		●	80 *0·99*	●	125 *7·11*	—		—		●

Table 1. (C) Transition temperatures (°C) and enthalpies (kJ/mol) of compounds **IC**.

$$H(CH_2)_n O - \bigcirc - COO - \bigcirc - CH_2 - CH_2 - \bigcirc - OOC - \overset{*}{C}H - CH_2 - CH - CH_3$$
$$\underset{Cl}{|} \quad \underset{CH_3}{|}$$

IC
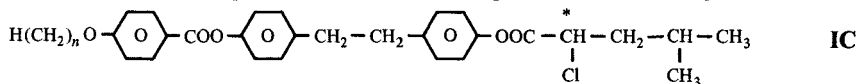
n	C		S_I^*		S_C^*		S_A		I
6	●	74 *16·1*	●	78 *1·56*	●	101 *0·06*	●	114 *4·26*	●
7	●	70 *19·4*	●	82 *1·69*	●	108 *0·15*	●	114 *5·28*	●
8	●	68 *34·87*	●	81 *2·96*	●	110 *0·08*	●	116 *10·1*	●
9	●	70 *21·3*	●	80 *1·3*	●	111 *0·04*	●	115 *6·2*	●
10	●	67 *22·4*	●	81 *2·2*	●	114 *0·08*	●	118 *6·8*	●
11	●	66 *23·8*	●	83 *2·56*	●	116 *0·11*	●	118 *7·4*	●
12	●	71 *27·1*	●	83·5 *3·51*	●	117·5 *0·05*	●	118·5 *8·05*	●

Table 2. Transition temperatures (°C) and enthalpies (kJ/mol) of compounds **II**.

$$H(CH_2)_nO - \langle O \rangle - CH_2 - CH_2 - \langle O \rangle - OOC - \langle O \rangle - OOC - \overset{*}{CH} - CH - CH_3 \quad (\overset{|}{Cl} \ \overset{|}{CH_3})$$

n	C		S?		S$_B$		S$_I^*$		S$_C^*$		S$_A$		N*		I	II
6	•	59	•	84	•	96	—		•	106	—		•	125	•	
		15·16		*0·134*		*3·48*				*0·70*				*1·93*		
7	•	69	•	96	—		—		•	110	•	111	•	122	•	
		19·25		*3·49*						*0·193*		*0·5*		*2·14*		
8	•	81	•	98	—		—		•	112	•	115	•	121·7	•	
		19·2		*3·8*						*0·14*		*0·96*		*2·37*		
9	•	49	—		—		•	96·5	•	114	•	117	•	120	•	
		10·4						*3·6*		*0·11*		*1·33*		*2·43*		
10	•	48	—		—		•	96	•	114	•	118	•	119·5	•	
		16·6						*3·6*		*0·13*		*2·01*		*3·97*		
11	•	57	—		—		•	95·5	•	114	•	119	—		•	
		20·0						*3·6*		*0·09*		*6·55*				
12	•	60	—		—		•	95·2	•	114	•	118	—		•	
		20·9						*3·66*		*0·05*		*6·63*				

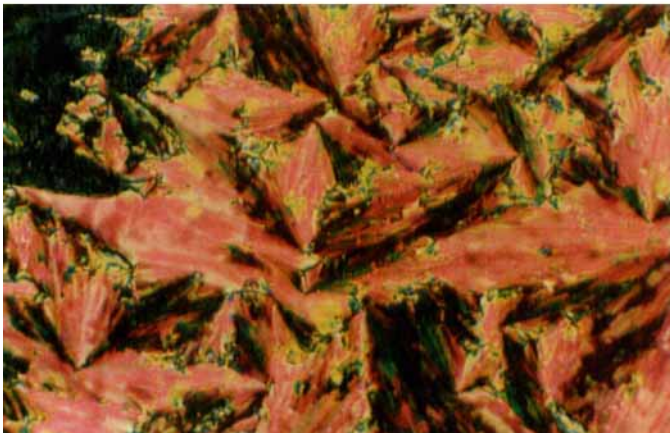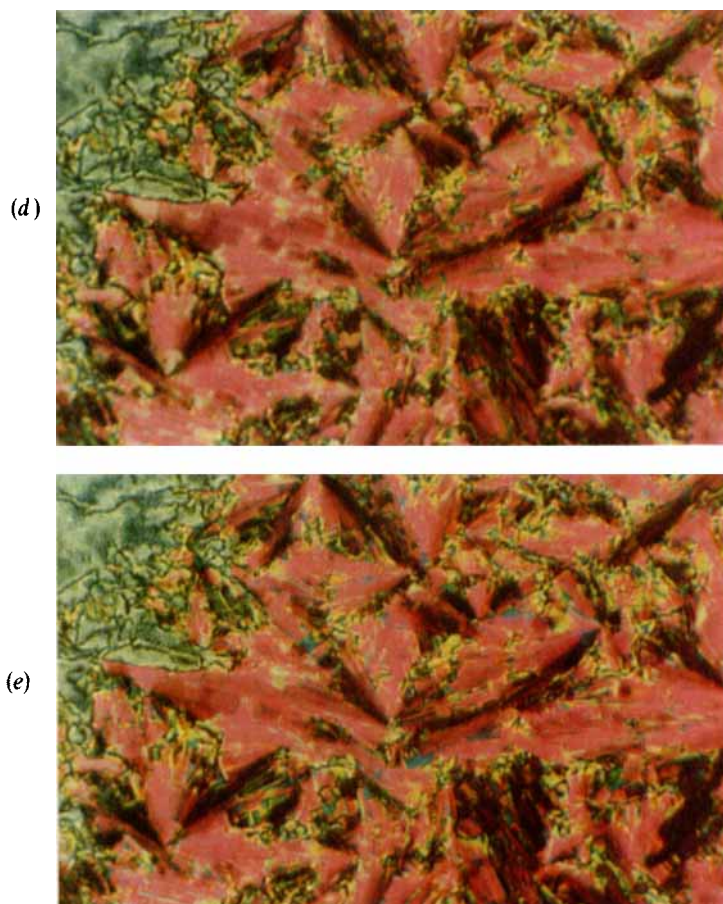H. T. Nguyen *et al.*

(*a*)

(*b*)

(*c*)

Figure 1.   Textures of mesophases formed by compound **IA** ($n=8$). (a) N* phase, (b) S_A phase, (c) S_C^* phase, (d) S_I^* phase, (e) S_F^* phase.
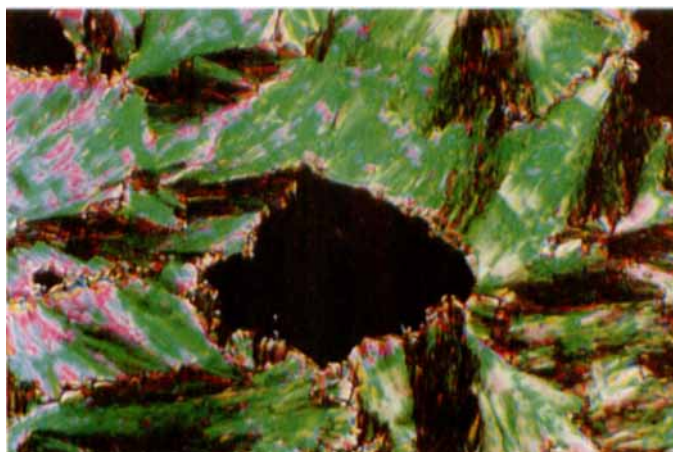

Figure 2.   Texture of the S_B phase of compound **II** ($n=6$).

Table 3.   Transition temperatures (°C) of compounds **III**.

$$C_9H_{19}O\!-\!\langle O \rangle\!-\!CH_2-CH_2-\langle O \rangle\!-\!OOC\!-\!\langle O \rangle\!-\!O(CH_2)_n-\overset{*}{\underset{\underset{CH_3}{|}}{CH}}\!-\!C_2H_5 \qquad \textbf{III}$$

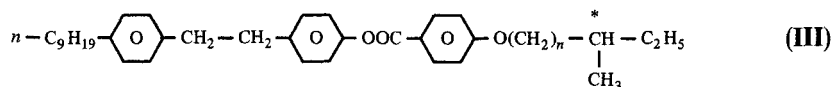| n		C		S_J^*		S_I^*		S_C^*		N*		I
3	•	65	•	82	•	95	•	111	•	123	•
4	•	60	•	79	•	93	•	111	•	118	•
5	•	72	•	82	•	99	•	121	•	123	•

2.2.3. *Series IC*

The characteristic feature of these compounds with a chiral chain derived from L-leucine, is the absence of a N* phase while S_A, S_C^* and S_I^* phases are observed for all the derivatives (see table 1 (C)). The melting and clearing temperatures are lower than those of **IA** and **IB** compounds.

2.2.4. *Series II*

This series is the isomer of series **IA**; the chiral chain being placed close to the benzoate group (the core has now been reversed). We must point out that the melting temperatures of these derivatives are very low, as seen in table 2. Two of them display the S_I^* phase between 48–49 and 96°C; they will be used for S_I^* mixture studies.

The first member ($n = 6$) of the homologous series is the only one that does not exhibit the S_A phase. On cooling from the isotropic liquid we can observe first the cholesteric phase (N*) with an oily streak texture. On further cooling, below the N* phase, an S_C^* phase appears with broken fan shaped or schlieren texture. At 96°C a S_B–S_C^* transition occurs; cooling the S_C^* leads to an S_B phase with a homeotropic texture in the preceding schlieren one. Moreover in the broken fan shape texture, bars appear and disappear (see figure 2). We note that in this series, two compounds exhibit the required sequence N* S_A S_C^* S_I^* ($n = 9$–10) for display device applications.

As for most of the derivatives of series **II**, the S_A phase is present only with a narrow range of temperatures of about 4°C, on the other hand, the compounds of the series containing chiral alkoxy chains **III** (see table 3)

$$n-C_9H_{19}\!-\!\langle O \rangle\!-\!CH_2-CH_2-\langle O \rangle\!-\!OOC\!-\!\langle O \rangle\!-\!O(CH_2)_n-\overset{*}{\underset{\underset{CH_3}{|}}{CH}}\!-\!C_2H_5 \qquad \textbf{(III)}$$

do not show a S_A phase at all. This behaviour was also reported by Kelly [6] in the series where the first phenyl ring was replaced by a cyclohexyl ring.

2.3. *Calorimetric study*

This study was performed with a DSC 7 Perkin–Elmer apparatus. All of the transitions could be detected in this study, even though the transition enthalpies of the N*–S_A and S_A–S_C^* transition could be very weak (see tables 1 (A), (B), (C) and 2):

The N*–I transition enthalpy is found between 1·3 and 4·0 kJ/mol and increases with the chain length.

The S_A–N* transition enthalpy is weak for the first members showing this transition. It also increases with the chain length.

The S_A–I transition enthalpy is higher than that of the other transitions (except the melting enthalpy). The average value is 6·3 kJ/mol.

The S_C^*–S_A transition enthalpy is the weakest one in this study varying from 0·015 to 0·16 kJ/mol (except the heptyloxy derivative of series **II** with 0·5 kJ/mol).

For the only compound (**IB**, $n = 12$) displaying a S_C^*–I transition, this enthalpy is comparable to that of a S_A–I transition.

The S_I^*–S_C^* transition enthalpy varies between 0·94 and 4·0 kJ/mol and the average value is about 2·1 kJ/mol similar to that of a N*–I transition.

The S_F^*–S_I^* transition is observed in three derivatives ($n = 6$–8) of series **IA**, its enthalpy decreasing as the chain length is increased (from 0·24 to 0·03 kJ/mol).

We could only measure one S_J–S_I^* and one S_B–S_C^* transition enthalpy; their values are respectively 1·05 and 0·15 kJ/mol.

The ΔH values of the corresponding melting transition turn out to be about 22·8 kJ/mol for the **IA, B, C** series and somewhat smaller for series **II**. This feature may be due to the low melting temperatures of **II**.

2.4. *Electrooptical properties*

We now consider the physical properties of these compounds, especially their response to an AC electric field and also their spontaneous polarization. For these experiments the so-called bookshelf geometry described by Clark and Lagerwall [2] was used. The liquid crystal was sandwiched between two crossed glass plates (70 × 160 mm) coated with tin oxide (30 Ω^2, Balzers). The planar geometry was obtained by coating both substrates with a thin layer (300 ± 50 Å) of polyvinyl alcohol whose polymeric chains were elongated in one direction by rubbing with a velvet cloth after curing. The thickness of the samples ($\sim 3 \, \mu$m) was checked with the Newton colours method. The cell was then placed in an oven controlled by an MKI system for INSTEC. Inc., allowing measurements with an accurate temperature control ($\pm 0.1^\circ$C).

The values of the spontaneous polarization were obtained by measuring the transient current induced by the switching of the dipole twice the tilt angle θ. We worked with the following conditions: a recurrence frequency of 3 kHz and an applied voltage increasing from 0 V to ± 40 V in order to obtain saturation of the polarization. This saturation is achieved at about ± 20 V. Another important characteristic of ferroelectric compounds is their response time to an electric field. The most relevant parameter can be defined as

$$\tau = \frac{\displaystyle\int_0^\infty i_p(t) \, dt}{2 i_p(\tau_s)},$$

where $i_p(t)$ is the current curve and τ_s is the time between the field reversal and the maximum of the current peak [7]. We believe this experimental quantity to be the most specific and also quite independent from boundary conditions of the measuring cell.

P and τ were measured as a function of temperature and of the applied voltage. Figure 3 shows P versus $T_c - T$ for three compounds of series **IA**, where T_c is the transition temperature between S_A and S_C^*, for a 10 V/μm applied field. The alkyl chain length was changed and, as expected, an increasing polarization was measured as the chain shortened. This may be attributed to the fact that the C_{11} derivative allows a
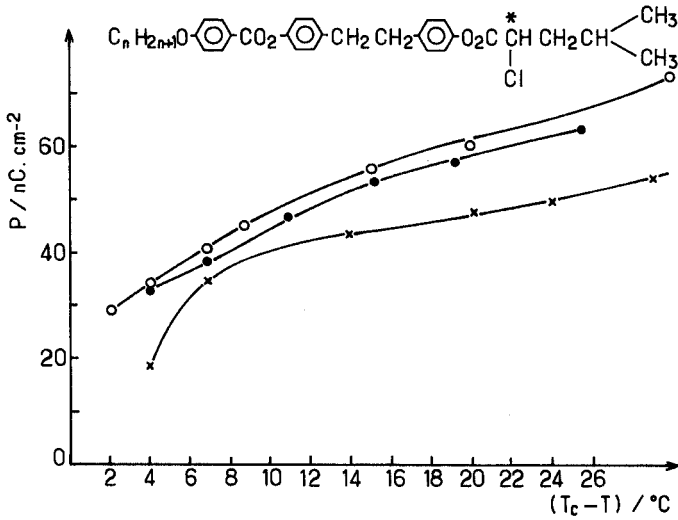
H. T. Nguyen *et al.*

Figure 3. The polarization P versus $T_c - T$ for three compounds of series IC $\bigcirc$, $n=8$; $\bullet$, $n=9$; $\times$, $n=11$.
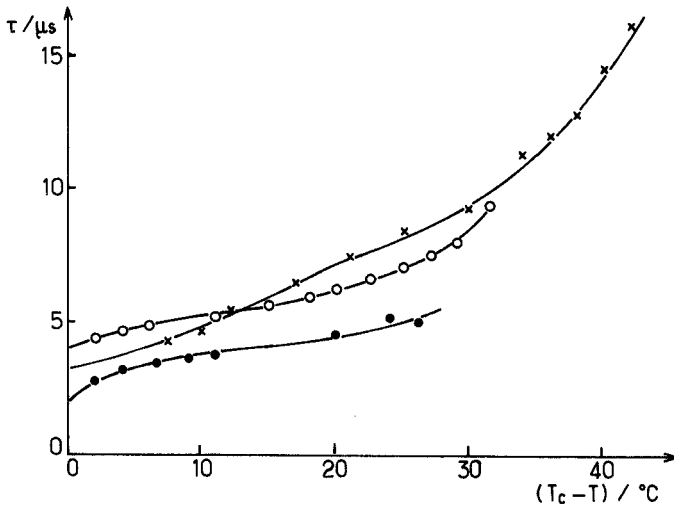
Figure 4. The response time τ versus $T_c - T$ for three compounds of series **IA** ($\times$, $n=8$), **IB** ($\bigcirc$, $n=8$), **IC** ($\bullet$, $n=8$).
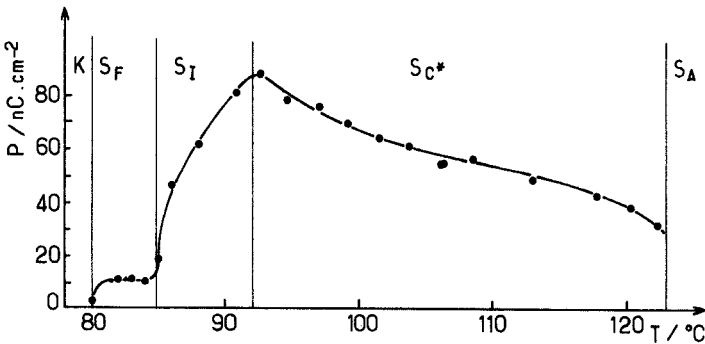

Figure 5. The polarization P versus T for compound **IA** ($n=8$).

quite unrestricted rotation of the molecules as compared to C_9 and C_8, thus tending to decrease the magnitude of P. The experimental response times for compounds **IA** ($n = 8$), **IB** ($n = 8$) and **IC** ($n = 8$) are reported on figure 4. In spite of the long core, these derivatives display a low response time, for example at ($T_c - T$) of 30°C, it is around $10\,\mu s$ ($\pm 10\,V/\mu m$).

We also investigated some compounds through all of their mesomorphic domain. For instance, the compound **IA** ($n = 8$) exhibits three ferroelectric phases S_C^*, S_I^*, S_F^* (see figure 5) P decreases from S_C^* to the crystalline phase but short range order in the smectic planes still gives rise to reasonable values for S_I^*. Response times, of course, in S_I^* and S_F^* are two or three orders of magnitude lower as compared to S_C^*, this is due to a more developed molecular ordering. An extensive study of the ferroelectric properties of these phases is in progress and will be published elsewhere.

2.5. X-ray diffraction measurements

X-ray diffraction patterns of powder samples of ferroelectric liquid crystal compounds in Lindemann capillaries were recorded photographically at several temperatures using a Guinier focusing camera equipped with a bent quartz mono-chromator (Copper $K\alpha_1$ radiation from a Philips PW-1009 generator) and an electrical oven. Figure 6 shows the variation of the layer thickness as a function of temperature for four compounds of series II through the different smectic phases. For all of the compounds, the layer thickness in the chiral smectic C phase increases as a function of increasing temperature, corresponding to a decrease of the tilt angle of the director. It has to be noted that this behaviour is true even though the S_C^* phase is not followed by a chiraa smectic A phase (for example with the $n = 6$ compound where the chiral smectic C phase transforms directly into a N* phase); usually, the tilt angle in a smectic C phase is independent of temperature when no smectic A phase occurs at higher temperatures. In the smectic B or I* phase, the layer thickness measured is compatible either with the molecular length (smectic B) or with a small tilt angle (chiral smectic I). The tilt angle, θ,
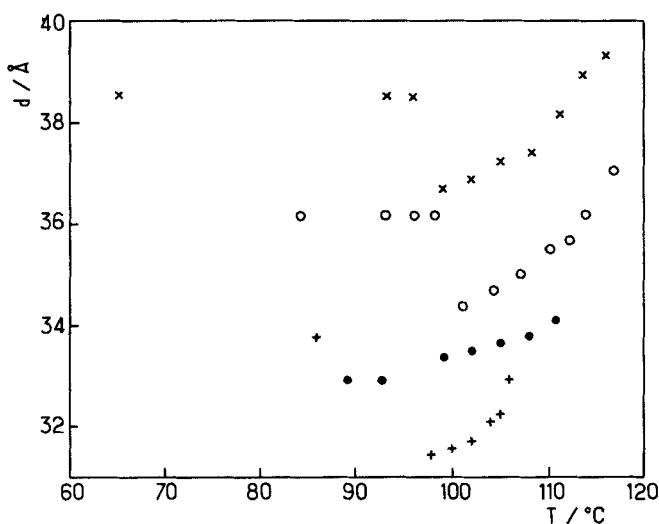

Figure 6.   The layer spacing as a function of temperature for compound **II** $+$, $n = 6$; $\bullet$, $n = 8$; $\bigcirc$, $n = 10$; $\times$, $n = 12$.
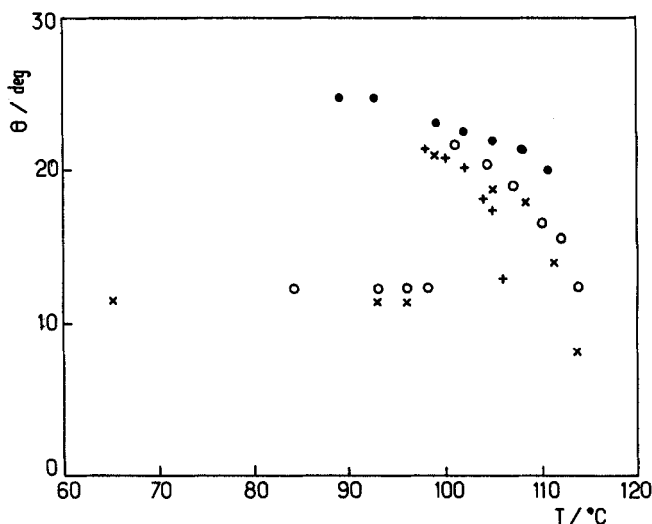
Figure 7. The tilt angle as a function of temperature within the chiral smectic I and C phases of compounds II +, $n = 6$; ●, $n = 8$; ○, $n = 10$; ×, $n = 12$.

of the director with respect to the smectic plane, is given in figure 7 as a function of temperature for the chiral smectic I and C phases. It has been determined by comparing the layer thickness measured experimentally to the length of the molecule as found by molecular modelling. In the chiral smectic I phase, θ is small (about 10° to 15°) in agreement with some other values already reported for this type of smectic phase [9]. On the other hand, the maximum tilt angle measured in the chiral smectic C phase is about 22° to 24°, which is the ideal value for display device applications.

Compound $n = 8$ of the IA series has also been investigated by X-ray diffraction. The layer thickness in the chiral smectic A phase at 129°C has been found equal to 34·9 Å in agreement with the molecular length ($\sim 34·5$ Å). In the chiral smectic C phase, the layer thickness is 32·5 Å at 120°C, then 30·9 Å at 100°C; thus the maximum tilt angle of the director seems close to 30°, lower than the value found for compounds of series II. In the chiral smectic I and F phases. The layer spacing is 30·9 Å at 90°C and 30·7 Å at 83°C respectively, the tilt angle being constant at about 28° in these two phases.

2.6. *Experimental*

Infrared spectra were recorded using a Perkin–Elmer 783 spectrophotometer and the NMR spectra with a Bruker 270 MHz. The microanalysis were performed by CNRS laboratory 'Service Central d'Analyse'.

2.6.1. *1,2-di(4-methoxyphenyl)ethane 2*

A solution of 51·2 g (0·2 mol) of desoxyanisoin 1 and 20 g (0·4 mol) of 55 per cent hydrazine hydrate was heated under reflux for 1 hour. Diethylene glycol (250 ml) and KOH (20 g, 0·357 mol) were added to the cooled solution. The mixture was heated gradually to 220°C, in the process distilling off the excess hydrazine hydrate. Then the solution was heated at this temperature until the evolution of nitrogen had ceased (3 hours). The cooled mixture was hydrolysed with water (500 ml) and the organic material was extracted with diethylether (3 × 300 ml). The combined organic fractions were washed with 10 per cent hydrochloric acid (300 ml), water (2 × 400 ml) and dried

(anhyd. Na_2SO_4). The solvent was evaporated and the product was recrystallized in absolute ethanol. The yield of 2 was 40 g (83 per cent), m.p. = 173°C. IR (Nujol): 1610, 1510, 1240, 830 cm^{-1}. NMR ($CDCl_3$, δ): 2·9 (s-4, 2 CH_2), 3·9 (s-6, 2 CH_3), 6·96–7·46 (two d-8 H Ar). Analysis: calculated for $C_{16}H_{18}O_2$: C, 79·34; H, 7·44; found: C, 79·29; H, 7·55.

2.6.2. *1,2-di(4-hydroxyphenyl)ethane 3*

A mixture of 40 g (0·17 mol) of 2 and 190 g (1·7 mol) of pyridine hydrochloride was heated at 220°C for 3 hours. The cooled solution was treated with a mixture of 40 ml conc. hydrochloric acid and 300 g crushed ice. The product was filtered off, washed with water and recrystallized in absolute ethanol. Yield: 29 g (80 per cent), m.p. = 199°C. IR (Nujol): 3380, 1615, 1600, 1510, 1240, 830 cm^{-1}. NMR (CD_3COCD_3, δ): 2·9 (s-4, 2 CH_2), 6·96–7·46 (two d-8 H Ar), 8·3 (s-2, 2 OH). Analysis: calculated for $C_{14}H_{14}O_2$: C, 78·50; H, 6·54; found: C, 78·26; H, 6·45.

2.6.3. *4-[β-(4-hydroxyphenyl)ethyl]phenyl 4-nonyloxybenzoate 4 (n = 9)*

A solution of 2·26 g (0·008 mol) of 4-nonyloxybenzoyl chloride (obtained from 4-nonyloxybenzoic acid with an excess of thionyl chloride) in toluene (100 mol) was added dropwise to a hot solution of 10 g (0·047 mol) of 3 and 20 ml of pyridine in 200 ml of toluene. The solution was refluxed for 2 hours and stirred at room temperature overnight. The solvent was evaporated under reduced pressure and the mixture was hydrolysed with 20 ml conc. sulphuric acid + 100 g crushed ice and 100 ml water. The solid was filtered off and was chromatographed on silica gel and eluted with the mixture toluene–ether (4 : 1) and recrystallized from absolute ethanol. Yield: 1·5 g (43 per cent), C 134°C N 142°C I. IR (Nujol): 3360, 1730, 1610, 1510, 1250, 840, 820 cm^{-1}. NMR (CD_3COCD_3, δ): 0·905 (t-3, CH_3 of C_9H_{19}), 1·3–2·2 (m-14, 7 CH_2), 2·9 (s-4, 2 CH_2 Ar) 4·3 (t-2, CH_2O), 6·9–8·2 (six d-12 H Ar), 8·35 (s-1, OH). Analysis: calculated for $C_{30}H_{35}O_4$: C, 78·26; H, 7·83, found: C, 78·36; H, 7·97. All the 4-[β-(4-hydroxy-phenyl)ethyl]phenyl 4-alkoxybenzoates 4 with alkyl chains C_6 through C_{12} were prepared in a similar fashion. The transition temperatures for the complete series are

C_6, C 130°C N 152°C I; C_7, C 134°C N 146°C I; C_8, C 131°C N 144°C I;
C_{10}, C 129°C N 140°C I; C_{11}, C 123°C N 136°C I; C_{12}, C 124°C N 133°C I.
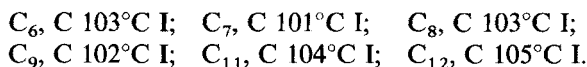
2.6.4. *4-[β{4-(2'S,3'S-2'-chloro-3'-methylpentanoyloxy)phenyl}ethyl]phenyl 4-nonyloxybenzoate 1B (n = 9)*

To a solution of 0·46 g (0·001 mol) of 4 (n = 9), 10 mg of 4-dimethylaminopyridine (DMAP) and 0·165 g (0·0011) mol of 2.S,3S-2-chloro-3-methylpentanoic acid in 3 ml of CH_2Cl_2 was added 0·226 g (0·0011 mol) of dicyclohexylcarbodiimid (DCC) at room temperature. The mixture was stirred overnight and filtered off. The solvent was evaporated and the solid was chromatographed on silica gel with toluene as eluent. The desired product was recrystallized in absolute ethanol. Yield: 180 mg (30 per cent). IR (Nujol): 1760, 1730, 1605, 1510, 1255, 840 cm^{-1}. NMR ($CDCl_3$, δ): 0·88 (two-4, CH_3 of $C_9H_{19}O$ and C_2H_5), 1·2–1·8 (m-18, 6.CH_2 of $C_9H_{19}O$, 1-CH_2 of C_2H_5 and CH–CH_3 of chiral chain), 2·9 (s-4, 2 CH_2–Ar), 4 (t-2, CH_2O), 4·4 (d-1, CH–Cl), 6·8–8·3 (six d-12 H Ar). Analysis: calculated for $C_{36}H_{45}O_5Cl$: C, 72·91; H, 7·59; Cl, 5·99; found: C, 72·54; H, 7·38; Cl, 6·12.

2.6.5. *4-[β-(decyloxyphenyl)ethyl]phenol 5 (n = 10)*

To a solution of 2·6 g (0·047 mol) of KOH, ethanol (200 ml) and 5 g (0·023 mol) of 3 at 90°C, was added dropwise a solution of 5·1 (0·023 mol) of 1-bromodecane in ethanol (100 ml). The mixture was refluxed for 3 hours. The solvent of the cooled solution was

evaporated and the mixture was hydrolysed with water (200 ml). The solid was filtered off, dried and chromatographed on silica gel with the mixture Hexane–Ether (7:3) as eluent. It was recrystallized in a mixture of Ethanol–Hexane (8:2). Yield: 3·2 g (40 per cent), m.p. = 103°C. IR (Nujol): 3370, 1610, 1510, 1250, 835, 830 cm^{-1}. NMR (CDCl$_3$, δ): 0·905 (t-3, CH$_3$ of C$_{10}$H$_2$O), 1·3–2·2 (m-16, 8 CH$_2$), 2·9 (s-4, 2 CH$_2$Ar), 4·1 (t-2, CH$_2$O), 7·0–7·7 (four d-8 H Ar). Analysis: calculated for C$_{24}$H$_{34}$O$_2$: C, 81·36; H, 9·60; found: C, 81·23; H, 9·64. All of the 4-[β-(4-alkoxyphenyl-ethyl]phenols with alkyl chains C$_6$ through C$_{12}$ were prepared in a similar fashion. The melting points for the complete series are

C$_6$, C 103°C I; C$_7$, C 101°C I; C$_8$, C 103°C I;
C$_9$, C 102°C I; C$_{11}$, C 104°C I; C$_{12}$, C 105°C I.

2.6.6. *4-[β-(4-decyloxyphenyl(ethyl]phenyl 4-(2S-2-chloro-3-methylbutanoyloxy) benzoate II (n = 10)*

To a solution of 0·71 g (0·002 mol) 5 (n = 10), 20 mg of DMAP and 0·57 g (0·0022 mol) of

$$CH_3-\underset{\underset{CH_3}{|}}{CH}-\underset{\underset{Cl}{|}}{CH}-COO-\left\langle\!\!\!\bigcirc\!\!\!\right\rangle-COOH$$
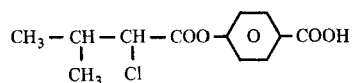
(prepared following the description in [8]) in 5 ml methylene dichloride was added 0·45 g (0·0022 mol) of DCC. The mixture was stirred over night. It was worked up and purified as previously to yield pure **II** (n = 10) (0·51 g, 43 per cent). IR (Nujol): 1760, 1730, 1600, 1510, 830 cm^{-1}. NMR (CDCl$_3$, δ): 0·9 (t-3, CH$_3$ of C$_{10}$H$_{21}$O), 1–1·9 (m-23, 8 CH$_2$ and CH(CH$_3$)$_2$), 2·9 (s-4, 2 CH$_2$–Ar), 4 (t-2, CH$_2$O), 4·4 (d-1, CH–Cl), 6·9–8·2 (six d-12 H Ar). Analysis: calculated for C$_{36}$H$_{45}$O$_2$Cl: C, 72·91; H, 7·59; Cl, 5·99; found: C, 73·01; H, 7·70; Cl, 6·03.

3. Conclusion

We have shown that the chiral diarylethane α-chloroester series display not only a ferroelectric S$_C^*$ phase but also ferroelectric S$_I^*$ and/or S$_F^*$ phases. In spite of the three benzene ring core, their response times are fast (around 10 μs at ($T_c - T$) of 30°C with a field of $\pm$ 10 V/μm). The spontaneous polarization of the S$_C^*$ phase is higher than those of S$_I^*$ and S$_F^*$. These compounds will be used for preparing different ferroelectric mixtures. Among all of the compounds reported in the present work, those of series **II** seem quite appropriate for display device applications, since they exhibit the ideal sequence of mesomorphic phases, namely N*, S$_A^*$, S$_C^*$, S$_I^*$, and also since the maximum tilt angle of the director in S$_C^*$ is about 22° to 24°.

References

[1] MEYER, R. B., LIEBERT, L., STRZELESKI, L., and KELLER, P., 1975, *J. Phys. Lett., Paris*, **36**, L.69.
[2] CLARK, N. A., and LAGERWALL, S. T., 1980, *Appl. Phys. Lett.*, **36**, 899.
[3] YOSHINO, K., and OGAKI, M., 1984, *Ferroelectrics*, **59**, 145.
[4] NGUYEN, H. T., ZANN, A., and DUBOIS, J. C., 1979, *Molec. Crystals liq. Crystals*, **53**, 43.
[5] KELLY, S. M., and BUCHECKER, R., 1988, *Helv. chim. Acta*, **71**, 451.
[6] KELLY, S. M., 1989, *Helv. chim. Acta*, **72**, 594.
[7] MARCEROU, J. P., LÉON, C., and DESTRADE, CH., *Ferroelectrics* (in the press).
[8] MOHR, K., KÖHLER, S., WORM, K., PELZL, G., DIELE, S., ZASCHKE, H., DEMUS, D., ANDERSON, G., DAHL, I., LAGERWALL, S. T., SKARP, K., and STEBLER, B., 1987, *Molec. Crystals liq. Crystals*, **146**, 151.
[9] GUILLON, D., SKOULIOS, A., and BENATTAR, J. J., 1986, *J. Phys., Paris*, **47**, 133.